

Design and automation of a pile test facility for offshore foundations and first experimental results

E. Weichhold, F. Dahlhaus
TU Bergakademie Freiberg, Germany

F. Adam
University of Rostock, Germany

T. Meier
Baugrund Dresden Ingenieurgesellschaft mbH, Germany

J. Großmann
GICON Holding GmbH, Germany

ABSTRACT: Offshore wind turbines (OWT) in deep-water sites of 50 meters and more require floating substructures. This paper will present a test facility for piles to be used for anchoring floating offshore substructures, in particular a Tension Leg Platform (TLP) substructure. Especially the measurement equipment, the loading cell, the controller technology and the automation will be highlighted. Another focus will be on the scaling laws for the pile and the soil. The paper will also provide an insight into the first experimental studies and their results. Beginning with the bracing types of the ropes between the piles and the OWT TLP substructure, there are two experimental set-ups. Firstly, piles loaded along longitudinal axis and secondly piles loaded with inclined forces transverse to the longitudinal axis. These scenarios are based on the specific loading from the buoyancy force, wave and wind loading. In this model test, the focus is on quasi-static pull-out tests with pulsating stress and cyclic tests with harmonic excitation.

1 INTRODUCTION

The continuous expansion of OWT, the increasing energy yield and capacity as well as the protection of coastal areas and the environment lead to offshore wind parks being constructed in further distance from shore and thus also in increased water depths. Water depths of 20 meter and more are often found in 10 to 200 nautical miles distance from the coastline.

In 50 to 200 m water depth, conventional bottom fixed offshore foundations such as monopiles, tripods, triple or jacket foundations are not economically viable. Alternative solutions are therefore required.

Such an alternative solution in form of a floating substructure for OWT in shallow as well as deep water is currently in development by GICON[®] GmbH and their partners. The combination of substructure and seabed foundation is based on the Tension Leg Platform (TLP) principle by Großmann et al. (2012), utilizing ropes.

Unlike piles of bottom fixed foundations which are subject to from significant compression and bending loads, the piles used for anchoring the GICON TLP is exposed to loads from permanent tensile forces, partly superimposed by a horizontal load. It should be noted that there are two types of loading regimes with respect to the loading direction. Firstly, loads along the longitudinal axis and secondly loads with inclined forces transverse to the longitudinal axis, see figure 1. Utilizing a pile test facility at a 1:15 scale, numerous

model tests under various load characteristics of the piles with different experimental arrangements and load spectra are being conducted at TU Bergakademie Freiberg in cooperation with industrial partners, in order to derive conclusions about the original state. In the following, the pile test facility will be presented in detail.

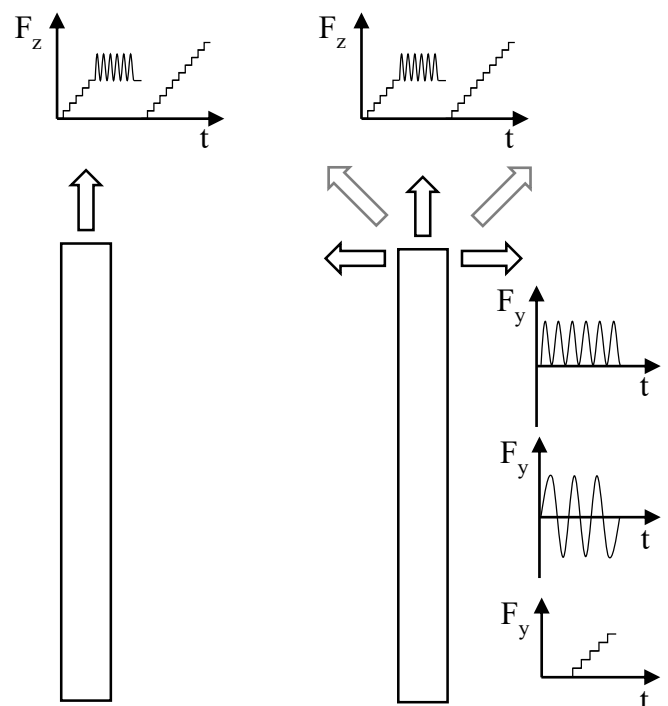


Figure 1. Experimental set-ups and loading regimes.



Figure 2. Pile test facility at TU Bergakademie Freiberg.
1) Measuring bridge 2) Platform, 3) Tank

2 DESIGN AND EQUIPMENT OF THE PILE TEST FACILITY

2.1 Test facility

The test facility consists of three basic components: measuring bridge (1), platform (2) and tank (3), see figure 2.

A pneumatic application of force, a support structure for attachment of position sensors and a camera are installed on the measuring bridge. The bridge is decoupled from the platform to provide a sufficiently dimensioned counter bearing for the tensile tests and to ensure that the test results are not influenced by movements of the platform and the tank.

The platform is used as a work platform at the time of the test and is equipped with a workstation for test management devices and data acquisition.

2.2 Measurement and control engineering concept

The test facility is equipped with sensors to measure temperature, strain, the displacement in the longitudinal axis of the pile and in the horizontal direction, air pressure and pore-water pressure.

Main components of the load units are pneumatic piston rod cylinders. For the load in the longitudinal

axis of the pile, a cylinder is connected to a piston with a diameter of $d = 160$ mm and a stroke length of $l = 50$ mm. Using a horizontally mounted cylinder with a piston diameter of $d = 80$ mm and a stroke length of $l = 100$ mm, any inclined forces transverse to the longitudinal axis can be generated in conjunction with the vertical cylinder.

A multifunctional data acquisition module by National Instruments allows for a reliable signal processing obtained from the sensors.

The digital processing and visualization of measurement data is performed using a program specially written for the test facility, based on the software 'LabView'; its user interface is characterized by the graphic display of the sensor signals and the unit for the pneumatic control.

The control of the pneumatic cylinder is implemented on the one hand by a software unit and on the other hand by pneumatic components, in particular a proportional pressure control valve in conjunction with electronic modules.

A target value for the pressure of the cylinder to retract is set via the software to the proportional control valve. By entering frequency, upper and lower pressure limit, a cyclic load with sinusoidal shape can be set.

Due to the inertia of the compressed air system, caused by overcoming the frictional force between the cylinder wall and piston rod and the relatively sluggish control of the proportional pressure control valve, an offset is created by setting the target value in the software to the reaction to the valve, and ultimately on the cylinder itself. This can result in a subsequent variation of the target value in positive or negative direction.

2.3 Selection of the pile material

Basis for modeling, especially with regard to the underlying forces, is the floating substructure for an OWT on a deep foundation. This type of deep foundation can be an alternative to the raft foundation planned for the pilot plant. Rammed steel piles are intended for the deep foundation; the pile diameters are about $D = 2500$ mm. The resulting moment of inertia of area I and the determined bending stiffness EI , with the modulus of elasticity E_{steel} from steel, are shown in Table 1 below.

A purely geometric scaling of the linear dimensions D , according to equation (3) with $\lambda = 15$ and $i = D$, leads to the likewise in Table 1 listed dimensions of the model pile. Also contained therein are values for I and EI with E_{steel} , determined from the scaled sizes, according to the equations (4) and (5).

$$i_M = \frac{i_P}{\lambda} \quad (3)$$

$$I = \frac{\pi \cdot \left(\left(\frac{D}{2} \right)^4 - \left(\frac{D}{2} - t \right)^4 \right)}{4} \quad (4)$$

$$EI = I \cdot E_i \quad (5)$$

The moments of inertia of area I_{xx} and I_{yy} , which vary due to different inner stiffening of prototype piles, cause minimal varied flexural strengths of loaded piles along the longitudinal axis.

Solf (2012) found that the mechanical influences often cause difficulties regarding the similarity considerations. Thus, the bending stiffness EI influenced the selection of the pile material during the preparation of tests with horizontally cyclic loaded piles.

Accordingly, there is a scaling with respect to the bending stiffness in accordance with equation (6):

$$EI_M = \frac{EI_P}{\lambda^5} \quad (6)$$

The starting points for scaling according to Solf (2012) are on the one hand, the linear dimensions of the model given in Table 1 and on the other hand, the bending stiffness of the pile - which is loaded with inclined forces transverse to the longitudinal axis - based on the moment of inertia of area I_{yy} as listed in Table 2 below.

The bending stiffness $EI = 8.54 \times 10^5 \text{ Nm}^2$ in Table 1 shows that with steel the desired bending stiffness of $EI = 1.40 \times 10^5 \text{ Nm}^2$ cannot be achieved; especially if a substantially complete similarity with the model pile's dimensions should be realized desired bending stiffness as per $EI = 1.40 \times 10^5 \text{ Nm}^2$.

This similarity can be achieved with a pile made of aluminum. It is easy to fabricate (sensor assembly) and has a low mass which makes handling of the pile easier.

Table 3 shows that a pile with a diameter of $D = 140 \text{ mm}$ and a wall thickness of $t = 2 \text{ mm}$, in conjunction with the elastic modulus of aluminum ($E_{\text{Alu}} = 6.90 \times 10^{10} \text{ N/m}^2$), results in a bending stiffness of $EI_{\text{Alu}} = 1.45 \times 10^5 \text{ Nm}^2$. This determines a model pile which is sufficiently similar in terms of mechanical as well as geometric properties to the scaled prototype.

Table 1. Geometric scaling of the prototype.

	D in mm	t in mm	E_{steel} in N/m ²	I in m ⁴
Prototype	2500.00	35.00	2.10×10^{11}	2.06×10^{-1}
Model	166.70	2.33	2.10×10^{11}	4.07×10^6
	EI in Nm ²			
Prototype	4.32×10^{10}			
Model	8.54×10^5			

Table 2. Mechanic scaling of the pile types.

	I in m ⁴	EI_{steel} in Nm ²	EI in Nm ²
Prototype vertical pile			
I_{xx}	2.48×10^{-1}	5.21×10^{10}	6.86×10^4
I_{yy}	2.81×10^{-1}	5.91×10^{10}	7.78×10^4
Prototyp3 diagonal pile			
I_{xx}	4.62×10^{-1}	9.69×10^{10}	1.28×10^5
I_{yy}	5.06×10^6	1.06×10^{10}	1.40×10^5
with $E_{\text{steel}} = 2.10 \times 10^{11} \text{ N/m}^2$			

Table 3. Geometric and mechanic scaling for choice of model pile.

	D in mm	t in mm	I in m ⁴	E_{steel} in N/m ²
Aluminum, completely geometrically scaled				
Model	166.70	2.33	4.04×10^6	2.83×10^5
Aluminum, iterative mechanical scaling				
Model	165.00	5.00	8.05×10^6	5.64×10^5
Model	150.00	3.00	3.74×10^6	2.62×10^5
Model	140.00	2.00	2.06×10^6	1.45×10^5

3 TEST MATERIAL

3.1 General remarks

In addition to the technical equipment of the pile facility, the test material is of essential importance. Baugrund Dresden (2014) examined the subsoil of the site where the planned offshore wind turbine is to be built on a floating substructure. The grain size distribution of the original soil shown in Figure 2 have been taken from this report.

The test material HB 33 from the Niederlausitz 'Hohenbocka' mining district is selected based on the findings from subsoil analysis and used as model subsoil which is similar to the prototype site's sand. This is evident from figure 2.

A scaling of the grain is not provided for the tests as a model adjustment takes place with the calculations at model level.

The model tests shall establish a basis for the validation of numerical models. These numerical models require to formulate the mechanical behavior of the test material with the help of constitutive equation. The hypoplastic soil model shall be applied here.

3.2 Studies on the material properties

From the studies on the material, the properties of Hohenbocka quartz sand HB 33 can be described as fine sand, medium sand and slightly coarse. This fine sand is as well as the original sand, closely graded. The results of the experiments are listed in Table 4.

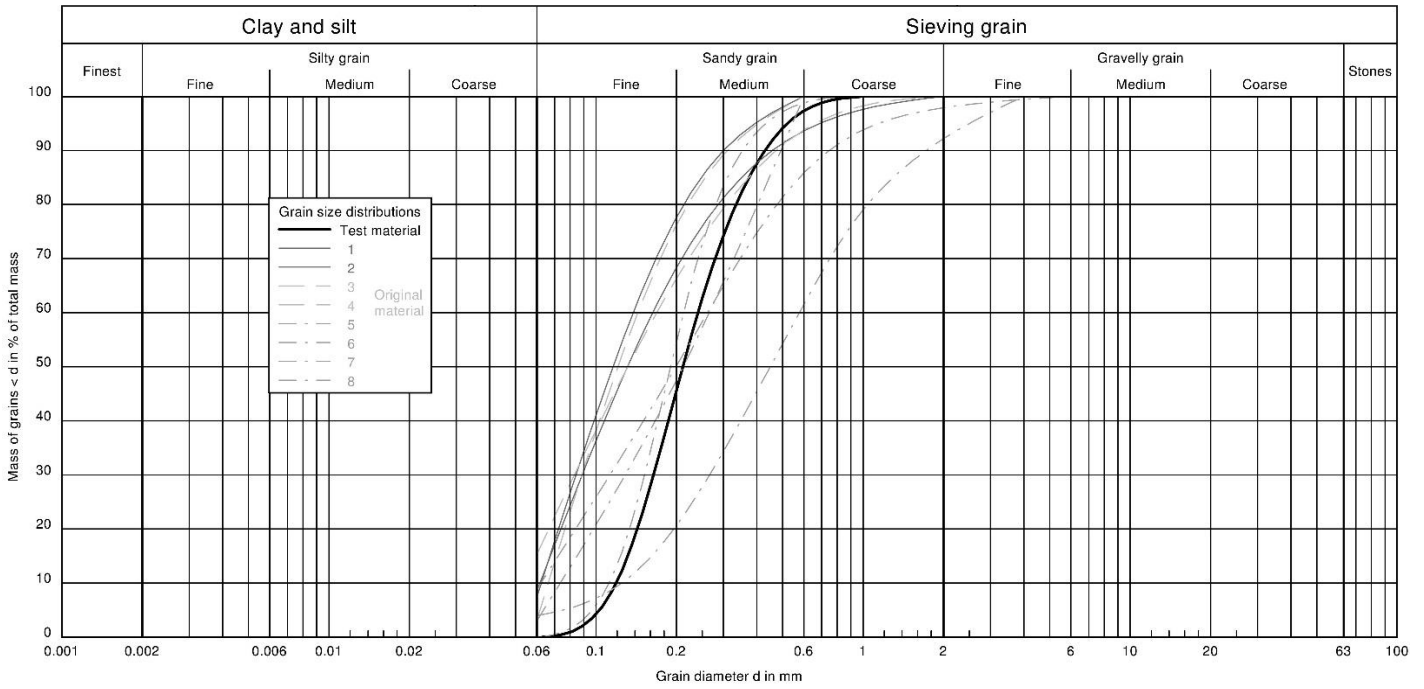


Figure 3. Grain size distributions of the original material (grey) and grain size distribution of the test material (black).

Table 4. Lab test results.

Property		Result
Soil type		msacsiFSa
coefficient of uniformity	$C_U / (1)$	2.0
Coefficient of gradation	$C_C / (1)$	0.9
Grain density	$\rho_s / (g/cm^3)$	2.6435
Loss on ignition	$V_{gl} / (\%)$	12.30
Minimum void ratio	$min e / (1)$	0.587
Minimum porosity	$min n / (1)$	0.370
Maximum dry density	$max \rho_d / (g/cm^3)$	1.666
Maximum void ratio	$max e / (1)$	0.934
Maximum porosity	$max n / (1)$	0.483
Minimum dry density	$min \rho_d / (g/cm^3)$	1.367

4 SAND AND PILE INSTALLATION METHODS

Loose and medium density to tight density conditions, under homogeneous conditions, are targeted requirements for the installation of the test material. Accordingly, the following installation methods, known from literature, are available:

- Pluviation method
- Layer based installation
- Sluicing method

The condition in the building for the experimental set-up and the test facility restrict the choice of installation methods. The experiment hall is not equipped with dust extraction equipment required for a dry installation. The gradual addition of dry sand is accompanied by dust development which should be avoided. As a result of the first installation, in which the test material was available in dry condition, and the non-existent option of drying the material, a renewed installation of dry material is not possible.

Moreover, installation of a trickle-in device at the dimensions of the test facility comes at a very high cost. Consequently, only layer based installation or sluicing method are possible.

Since vibrations and tremors from ramming operations need to be avoided to prevent damage to the sensors, this type of pile installation cannot be selected.

5 TEST PROCEDURE

5.1 Experimental set-up

As per Adam et al. (2014), there are two types of loadings for the piles: one axially loaded in the direction of the longitudinal axis of the pile and a pile which is additionally exposed to stress transverse to the longitudinal axis. These types of bracing of the ropes lead to two principal experimental set-ups, see figure 1:

- Experimental set-up with piles loaded along longitudinal axis
- Experimental set-up of piles loaded with inclined forces transverse to the longitudinal axis

In both experimental set-ups the pile is exposed to different load scenarios. In the model, this will be represented by quasi-static pull-out tests with pulsating stress and cyclic tests with harmonic excitation.

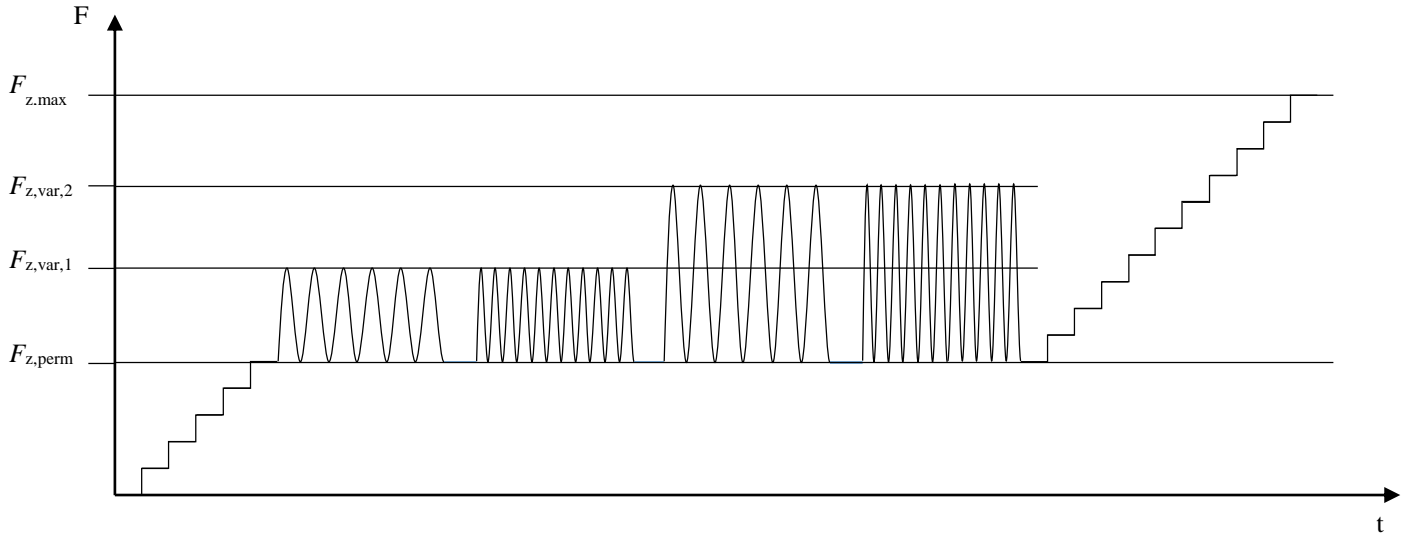


Figure 4. Schema of the load programme for the force along longitudinal axis of the pile.

5.2 Software and programme

Basis of the test programme are the results of a numerical simulation calculation using ANSYS software. Details of the calculations and assumptions can be found in Adam et al. (2014).

The calculations with ANSYS provide characteristic loads on the two principal pile types, represented in a line model, which are subjected to the load cases DLC 1.2 and DLC 6.1 according to DIN EN 61400-1:2011 and DIN EN 61400-3:2010.

The load cases DLC 1.2 and DLC 6.1 considered loads with respect to the wind direction at 0° (main wind direction) and 45° . In load case DLC 6.1 with ice, a wind load at 22.5° is assumed.

The forces from three-dimensional coordinates x , y and z are considered. In experiment set-up A, the forces to consider are only F_z along the longitudinal axis of the pile.

The resulting force F_{res} from horizontal (F_y) and vertical ratio (F_z) is however prevailing in experiment set-up B.

The critical loads for both experimental arrangements are provided regarding the pile which attains the respective maximum value for F_z respectively F_{res} in the calculation results. In Table 5, exemplary loads are listed for the model tests.

With the aid of scale factor λ^3 for a force F according to Chakrabarti (2005), equation (7) provides the applicable law for scaling the loads on the model scale.

$$F_{i,M} = \frac{F_{i,P}}{\lambda^3} \quad (7)$$

For the experimental arrangements the following load spectra are used and which is shown as schema in figure 1:

- Experimental set-up A
 1. quasi-static load increase on permanent load $F_{z,perm}$
 - a) quasi-static loading with pulsating stress between $F_{z,perm}$ and $F_{z,var}$ to $F_{z,max}$
 2. quasi-static load increase on $F_{z,max}$
- Experimental set-up B
 1. quasi-static load increase on permanent load $F_{z,perm}$
 - a) quasi-static loading with pulsating stress between $F_{z,perm}$ and $F_{z,var}$ also $F_{y,perm}$ and $F_{y,var}$ to $F_{res,max}$
 - b) quasi-static loading with pulsating stress between $F_{z,perm}$ and $F_{z,var}$ under cyclic stress of F_y
 2. quasi-static load increase on $F_{z,max}$ and $F_{y,max}$

The experiment with pulsating stress has the focus that the pile is charged cyclically between a lower and upper limit of a particular load $F_{z,i}$. Under certain circumstances, this can result in pull-out of the pile, respectively a vertical displacement of the pile head.

Via quasi-static stress the system is loaded in the first part up to a load $F_{z,perm}$, which sets the lower limit in the subsequent pulsating test portion. The upper limit is given by $F_{z,var,1}$, see figure 4.

The experiments in experimental set-up B provide a gradual increase in load $F_{res,var}$ to maximum variable force $F_{res,max}$. As in experimental set-up A-1, the load between $F_{res,perm}$ and $F_{res,var,i}$ is done cyclically.

The experimental programme of the first tests has variations with regard to type of load, force and frequency.

The following exposure frequencies were investigated: $f_1 = 0.1$ Hz, $f_2 = 0.5$ Hz and $f_3 = 1.0$ Hz. The experiments were performed with a minimum of 100 and a maximum of 1000 cycles.

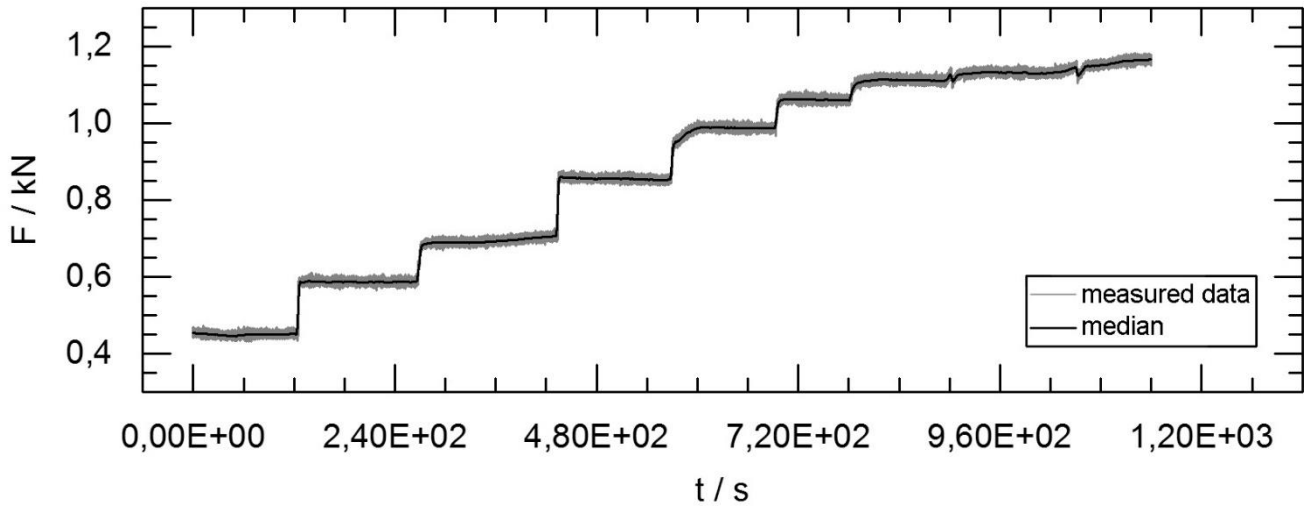


Figure 5. Force-time curve – quasi-static pull-out test.

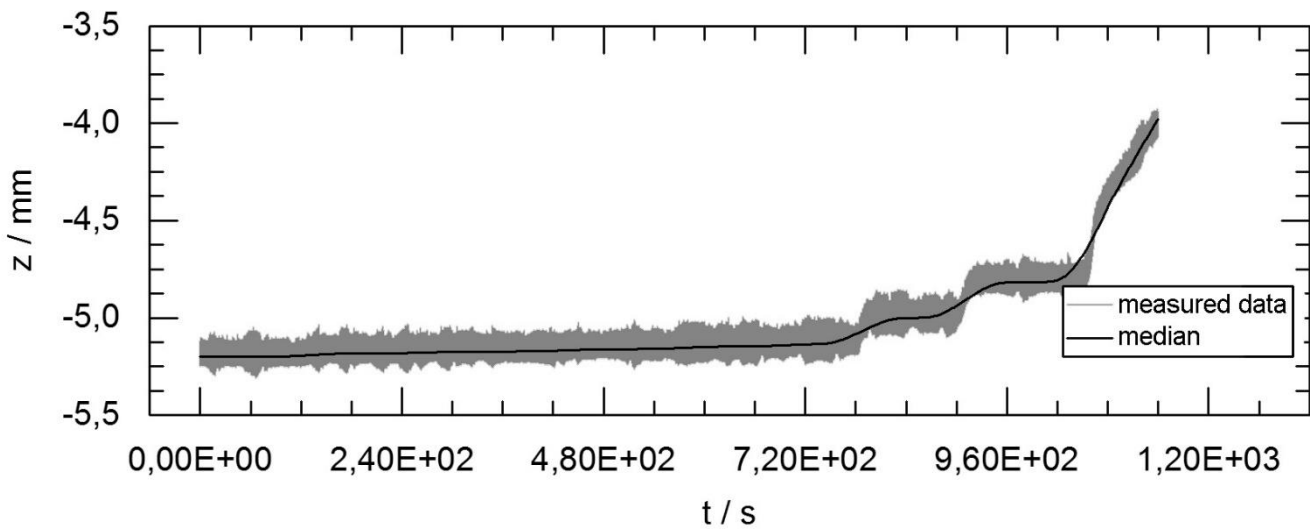


Figure 6. Path-time curve – quasi-static pull-out test.

The criterion for discontinuation of the experiment was determined by the displacement of the pile with too high a value. For future trials which are not part of this paper, a termination criterion at a vertical displacement of a maximum of $z = 2.0$ mm is recommended.

Table 5. Exemplary loads.

	Prototype / MN	Model / kN
Loads for setup A; from load case DLC 6.1 with wind direction of 45°		
$F_{z,max}$	6.016	1.783
$F_{z,per}$	1.514	0.449
$F_{z,var}$	4.502	1.334
Loads for setup B; from load case DLC 6.1 with wind direction of 0°		
$F_{y,max}$	2.771	0.821
$F_{y,per}$	0.000	0.000
$F_{y,var}$	2.771	0.821
$F_{z,max}$	2.935	0.870
$F_{z,per}$	1.865	0.553
$F_{z,var}$	1.070	0.317
$F_{res,max}$	4.036	1.196
$F_{res,per}$	1.865	0.553
$F_{res,var}$	2.171	0.643

6 EXPERIMENT EVALUATION AND FIRST RESULTS

The experiments are evaluated on the basis of the sensor signals. Thus, there are investigations into the behavior of force and displacement, the change in length, the pore-water pressure and the temperature. The evaluation also includes the frequency and force ranges.

Figures 5 and 6 show exemplary force-time and path-time curves of the quasi-static pull-out tests like experimental set-up A-2

6.1 Force and displacement

The force curve of quasi-static tests to permanent force $F_{z,perm}$, as shown in Figure 3 corresponds to the planned force progression. The displacements due to the load have minimal changes to $\Delta z = 0.03$ to 0.05 mm.

The part experiments with pulsating load consisted of the load regime from a quasi-static and variable

load, as can be seen in Figure 4. Thus initially a static load increase to permanent load $F_{z,perm}$ occurs and then the variable load portion $F_{z,var}$ has to be gradually increased. The system is to be loaded at individual steps $F_{z,var,i}$ with the different frequencies.

Two partial experiments resulted in displacements of up to $\Delta z = 1.65$ mm and were terminated after 30 cycles.

The load behavior in all experiment parts is in accordance with the specifications. Due to the large displacements, particularly among the low frequencies, it was decided not to continue the experiments under pulsating load.

At this point, quasi-static pull-out tests were exclusively performed, as also seen in figure 4. The hereby applied load stages are clearly visible in the force progression, see figure 5.

The review of the displacement for example in figure 6, during one of the two quasi-static experiments shows a clear trend. Between the initial four load steps, only small changes in terms of displacement are observed. Between the fourth and fifth load stage, the displacements have a value corresponding to the preceding stages. At level 5, respectively 6, large, constant displacements occur. In both experiments, a load with $F_z = 1.2$ kN led to the permanent pull-out of the pile.

6.2 Length variation

The strain measurements show a stress ensuing behavior. The changes in length, viewed along the longitudinal axis of the pile, decrease with the distance from the load source. That means that length variations in the upper area are always higher than in the lower area.

The high sensitivity of the sensors at minimal impact prevents specific evaluation of the change in length as a result of a momentary load change, as was the case during the above-mentioned test series.

6.3 Conclusion

A significant aspect of the experimental control was that the pressure area limits had to sometimes be adjusted when changing the frequency. For example, an increase from f_2 to f_3 during to test segments resulted in increase of the upper pressure limit as well as a lowering of the lower pressure limit by respectively $\Delta p = 0.02$ bar.

It should be mentioned that each experiment, especially the cyclical experiment parts is preceded by an adjustment phase. In this phase, the lower limit is initially set and then the upper limit in accordance with the test requirements in terms of load ranges is adapted. Depending on the reaction of the valve and the cylinder, the duration of this phase varies. Both effects can be attributed to the previously mentioned system inertia.

7 ACKNOWLEDGMENTS

At this point we would like to express our special gratitude to the Federal Ministry for Economic Affairs and Energy of the Federal Government of Germany, for the financial support in the context of a project of the Central Innovation Programme for small and medium-sized enterprises (ZIM; KF2652106JA4). We also like to thank our partner GICON GmbH, ESG GmbH - a member of the GICON-group - and BAUGRUND Dresden Ingenieurgesellschaft mbH which support this project.

8 REFERENCES

- Chakrabarti, S. K. 2005. Physical Modelling of Offshore Structures. In S.K. Chakrabarti (ed.), *Handbook of offshore engineering: 1001–1054*, Amsterdam and London: Elsevier.
- DIN EN 61400-3 2010. Windenergieanlagen - Teil 3: Auslegungsanforderungen für Windenergieanlagen auf offener See, Deutsches Institut für Normung e.V (ed.).
- DIN EN 61400-1 (2011). Windenergieanlagen - Teil 1: Auslegungsanforderungen, Deutsches Institut für Normung e.V (ed.).
- Großmann, J. et al. 2012. The GICON® SOF: A Tension Leg Platform development for various offshore conditions, combining proven technology and innovation. *Renewable UK, Global Offshore Wind, 13./14. June 2012, London*
- Solf, O. 2012. Zum mechanischen Verhalten von zyklisch belasteten Offshore-Gründungen, Karlsruhe: KIT, 2011
- Adam, F. et al. 2014. *Evaluation of internal force superposition on a TLP for wind turbines*. *Renewable Energy* 71: 271-275.
- Baugrund Dresden 2014. Ergebnisbericht zu den Baugrunduntersuchungen. In Baugrund Dresden Ingenieurgesellschaft mbH (ed.), *Projektunterlagen*. Dresden.